Dual-Band Complementary Split-Ring Resonator (CSRR) with High-Quality Factor and Its Applications in Low Phase Noise Oscillators and Small Multi-Band Diplexers and Filters

Mehdi Hamidkhani* and Farzad Mohajeri

Abstract—Low-Loss resonators with high Q factor have special importance in modern microwave telecommunications systems. In this paper, a modern dual-band CSRR with high Q factor is first examined using SIW technology on a surface waveguide. It should be noted that the proposed structure paves suitable way for emitting and propagating wave in two passing bands (approx. 4.7 and 5.3 GHz) below cutoff frequency waveguide. High Q factor and its high small-sized percentage is the salient specification of this structure as compared to other similar planar resonators proposed in various references.

At the end of this paper, three applications of this resonator are studied in designing a small multi-band filter with high Q factor, a small multi-band diplexer with low passage bandwidth and a planar oscillator with low-phase noise. According to the scientific literature, the proposed oscillator was found to enjoy the best performance at low phase noise for planar microwave oscillators.

1. INTRODUCTION

Metamaterials are one of widely-used samples in electromagnetics. They have already led to the unprecedented microwave applications [1]. One of these important applications is using metamaterials in designing resonators. Split ring resonator (SRR) and its dual, complementary split ring resonator (CSRR) have been introduced as key components to synthesize metamaterial microstrip lines with negative permittivity, which support a forward-wave or backward-wave passband [2, 3].

In this paper, waveguide structures are selected in order to apply the metamaterials. The first reason is that waveguides show high Q factor which can be used in designing low loss and noise components with a good power handling capability. The second reason is that waveguides are able to provide negative permittivity when operated below the cutoff frequency of the dominant TE mode [3–7]. Since CSRRs show negative permittivity, using these resonators into waveguide will lead to positive permittivity factor below cutoff frequency of main mode. Accordingly, a forward-wave passband below the cutoff frequency is achieved.

Since combination of CSRRs with a traditional metallic waveguide is difficult, substrate integrated waveguide (SIW) technology is used, which is a very suitable type of planar guided-wave structures. This technology is produced on a planar substrate with linear periodic arrays of metallic vias based on the printed circuit board (PCB). A structural sample along with required relation, in which SIW technology is used, is shown in Figure 1 [3–8].

Group delay is one of the salient specifications of each electronic and telecommunications system. As a matter of fact, group delay is defined as phase distortion of device, transition time of a signal through a device versus frequency and the derivative of the device's phase characteristic with respect to frequency. Therefore, group delay is defined as the negative derivative of the DUT's[†] phase characteristic
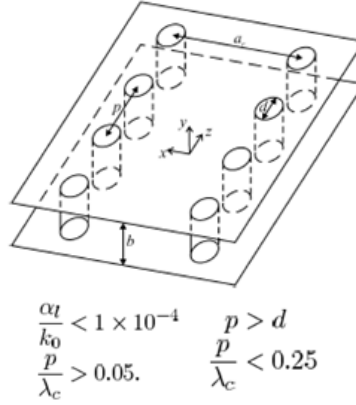
* Corresponding author: Mehdi Hamidkhani (mehdi.hamidkhani@gmail.com).

The authors are with Shiraz University, Iran.

† Device Under Test.

$$\frac{\alpha_l}{k_0} < 1 \times 10^{-4} \qquad p > d$$
$$\frac{p}{\lambda_c} > 0.05. \qquad \frac{p}{\lambda_c} < 0.25$$

Figure 1. SIW technology.

versus frequency as follow equation:

$$\tau_d = -\frac{1}{360} \cdot \frac{d\varphi}{df} \tag{1}$$

where τ_d is the group delay, f the frequency and φ the phase of S_{11} or S_{21} in degree. It should be noted that group delay is correlated with reflection coefficient which is called as devices group delay. Moreover, group delay can be correlated with transmission coefficient which is called as transmission (or insertion) group delay. The external quality factor related to the group delay of the device and insertion can be calculated through the following Equations (2) and (3):

$$Q_{ed} = \frac{\omega_o \cdot \tau_{s11}(\omega_o)}{4} \tag{2}$$

$$Q_{ei} = \frac{\omega_o \cdot \tau_{s21}(\omega_o)}{2} \tag{3}$$

where ω_o is the angular frequency [9]. Details of designing a modern dual-band CSRR with high Q factor are put forward. This resonator operates below initial cutoff frequency waveguide which leads to a small-sized. The salient specifications of the proposed structure include: low insertion loss, high miniaturizing percentage and high group delay in passband which causes high Q factor. In the end of this paper, three applications of this resonator are investigated in designing a multiband small filter with high Q factor, a small multiband diplexer with rather low bandwidth and a planar oscillator with low-phase noise.

The phase noise acts as a restriction factor for the performance of radar and telecommunication systems, and therefore, it is one of the most important parameters to be measured for oscillators. A resonator or a filter of high quality factor serves as the most critical component of a low phase noise oscillator. Many techniques and methods proposed for low phase noise oscillators employ the same basis. That is to say, they mostly place their focus on improving the feedback network features (resonators or filters) to consequently boost the phase noise [10–19].

2. THE PROPOSED CSRR RESONATOR CONFIGURATION

The proposed CSRR structure using SIW technology is shown in Figure 2, which includes two linear arrays of metalized vias (as electric side walls of the waveguide) in a substrate of Rogers RT/Duroid 5880 with a thickness of 0.508 mm and a pair of non-uniform ring slots located and etched on the metal cover of the waveguide. In order to eliminate any gap in the design frequency band, reduce scattering losses and ensure ease of fabrication, the diameters of these vias and a center to center spacing are optimized to 0.8 mm and 1.4 mm values, respectively. A 50 ohm microstrip feed line is used. The width of the waveguide is 11.5 mm which leads to the cutoff frequency of the initial SIW at about 8.7 GHz.

Furthermore, values for width and length of the waveguide (i.e., size of SIW) are dictated in two ways. Firstly, any decrease in width of the waveguide leads to increased cutoff frequency and miniaturization factor. However, this only influences the coupling while there is much less influence on the passband below the cutoff. Secondly, coupling is controlled by waveguide length within CSRR and input microstrip (L parameter in Figure 2). In addition, increased waveguide length has an increasing effect on the amount of loss. More specifically, there is a trade-off between lower loss and higher coupling during the adulation of waveguide length, while both of them are effective in having a resonator with high Q factor. Moreover, passbands are not influenced significantly by change in values of width and length of the waveguide. Nonetheless, increase in values of these two parameters leads to decreased cutoff frequency of the initial waveguide.

As displayed in Figure 2, the proposed structure is realized by incorporating two integrated pairs of non-uniform single-ring CSRRs on the metal surface of the waveguide. In terms of the direction of the split of the ring slot, they are back to back oriented. This alignment allows strong coupling between the waveguide and the CSRRs since the electric field reaches maximum in the waveguide center. The two single-ring CSRRs offer two relatively independent resonance frequencies.

The position of two bands can be independently controlled by changing their resonance frequencies. There are several factors that affect the self-resonance frequency of the CSRR, for instance, the length of split which can be used to adjust the frequency. The slot length and slot width are the two main parameters that determine the resonant mode.

Shape and dimensions of ring slots have been designed in such a way that one passband below waveguide cutoff frequency will be provided in each ring slot. In fact, the ring slot size can be determined according to the passband location. Each passband contains one pole and one transmission zero near each other. Nearness of pole and transmission zero leads to a sudden change in transition phase with small changes in frequency meant to have high group delay in each passband.

Moreover, dimensions of ring slots are optimized in such a way that two passbands should be placed near each other. Under such circumstances, second passband will be specified between two poles. Therefore, we will face a significant increased group delay in the second passband. Thereupon, since group delay and Q factor have direct relationship with each other, attaining a dual-band resonator
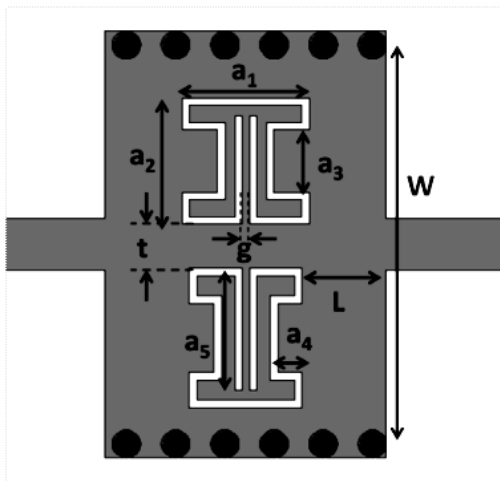
Figure 2. Configuration of the proposed SIW cavity CSRR filter. The geometrical parameters are $L = 2.2\,\text{mm}$, $g = 0.2\,\text{mm}$, $a_1 = 3.6\,\text{mm}$, $a_2 = 3.6\,\text{mm}$, $a_3 = 1.8\,\text{mm}$, $a_4 = 1.2\,\text{mm}$, $a_5 = 3.1\,\text{mm}$ for the upper CSRR and $L = 2.4\,\text{mm}$, $g = 0.2\,\text{mm}$, $a_1 = 3.2\,\text{mm}$, $a_2 = 4\,\text{mm}$, $a_3 = 2\,\text{mm}$, $a_4 = 0.9\,\text{mm}$, $a_5 = 3.5\,\text{mm}$ for the lower CSRR and $W = 11.5\,\text{mm}$, $t = 1.3\,\text{mm}$.
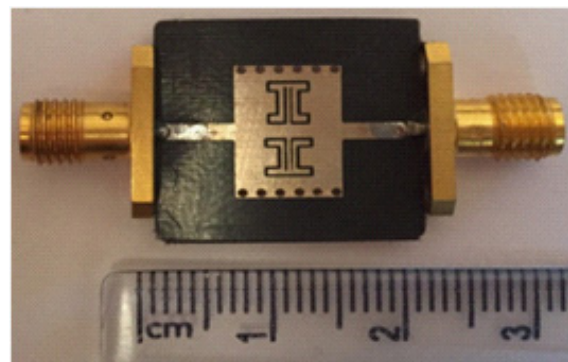

**Figure 3.** Image of the fabricated CSRR resonator.

with high Q factor in each two passbands especially second passband is possible.

Although there is high possibility of attaining group delay, destructive effects of insertion losses are impeded. In other words, there is the possibility of getting closer transmission zero and pole by adjusting the dimensions of ring slots. But in this case, firstly, change in transition phase versus frequency is increased which is meant to have high group delay. Secondly, pole is located closer to the pass band that is effective in increasing insertion losses. As a matter of fact, there is a trade-off between increased group delay and reduced insertion losses in passband. Here, attaining maximum possible group delay (which is equivalent to the maximum possible quality factor) has been considered in the design in order to have insertion losses lower than 2 dB. Finally, this resonator is constructed after optimization. The constructed sample is shown in Figure 3.

The results of simulation (were employed in HFSS software), measurement and circuit model for group delay and transmission responses of this resonator are shown in Figures 4 and 5. The simulation and measurement results are in relatively good agreement. Minor deviations between them arises from not-so-sufficient accuracy in the manufacturing process. As specified, this resonator contains two passbands in the frequencies approx. 4.7 and 5.3 GHz. It should be noted that group delay in these two frequency bands stands at approx. 4 and 23 ns, respectively, while insertion losses in these two frequency bands stand at about 0.5 and 2 dB, respectively. Of course, as mentioned, further group delay can be attained regardless of losses. For example, there is possibility of a group delay of more than 30 ns and insertion loss of 3 dB by changing the dimensions of ring slot. In this case, the insertion losses can be compensated by adding an active part (transistor).

(a)   (b)
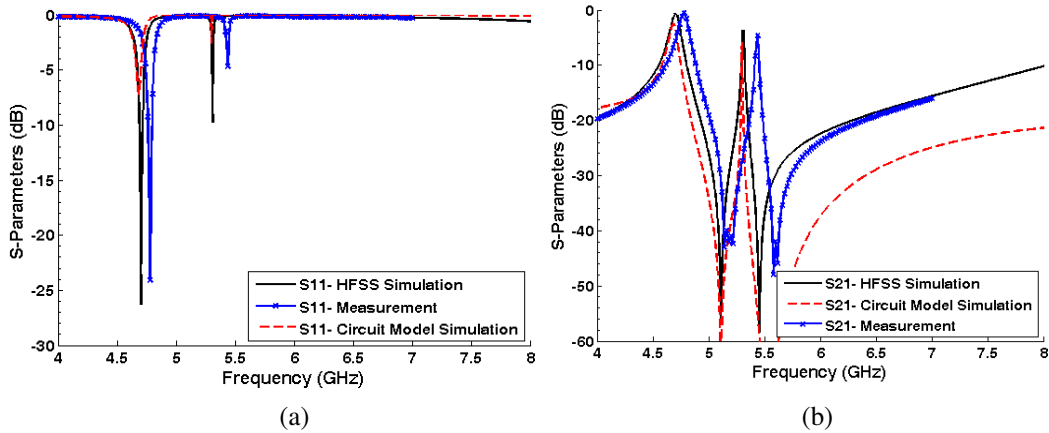
Figure 4. Measured and simulated transmission responses of the proposed CSRR resonator; (a) S_{11} parameter and (b) S_{21} parameter.
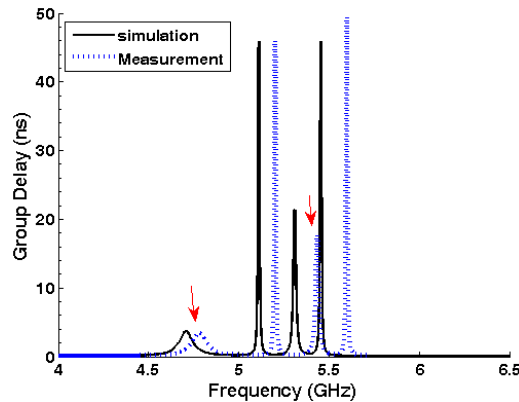

Figure 5. Simulated and measured transmission group delay corresponding to the proposed CSRR resonator.

The results show maximum unloaded Q factor which is equal to approx. 1800 for the second band with insertion losses lower than 2 dB and approx. 2500 with insertion losses lower than 3 dB. Therefore, this resonator is very suitable for designing a narrow multiband filter or a low phase noise oscillator. Especially in a low phase noise oscillator, there is an active part, and insertion losses of the resonator can be partly compensated. Also it should be pointed out that when the split of the ring slot is narrow, the unloaded Q-factor of the CSRR will be increased leading to a smaller bandwidth.

Once we intend to have a comparison with the structure proposed in [3] (the main reference of this paper for designing resonator), firstly, basic structure proposed by Itoh et al. is a single band, and secondly, group delay approx. 4 ns with insertion losses higher than 1 dB can be attained in that structure.

It should be noted that equivalent circuit model corresponding to this resonator, which is observed in Figure 6, is presented with the aim of better designing and, most importantly, to illuminate the essential differences between the ring slots which lead to the variations in transmission characteristics. In this simple model, material losses are ignored. In the same direction, SIW technology's pins can be considered as a short connection stub form which is modeled with "L_d" inductor. Ring slots can be modeled with a resonance source that is made of inductor and capacitor (C_r and L_r) with the parallel connection. The inductor connection of gap between waveguide transmission line and ring slot is considered in the form of "L_c" while capacitor connection between them is considered in the form of "C_c". Coupling between ring slots is modeled in the form of a resonance source using "L_s" and "C_s" [2].

It is important to note that these circuit models are indeed simplified versions. Here, three reasons explain the simplicity of this model. First, the via-walls are just represented by an inductance L_d. In fact, they should be modeled by infinite number of shunt inductances along the two-wire transmission line. Second, the CSRRs are coupled to the ground through both an equivalent inductance and a small capacitance C_2 in a parallel form. Impedance value of this parallel form is much lower than that of SIW vias (L_d). Thus, this impedance is neglected in order to simplify the model. Actually, CSRR and ground are put in direct connection with each other. Third, the distributed series inductance and distributed shunt capacitance of the waveguide are all neglected. Thus, the proposed circuit models are valid only for a limited frequency range. However, they are basically correct and fully capable of explaining the transmission characteristics of these structures.
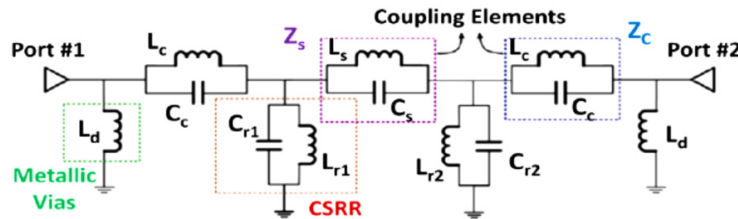
Figure 6. Equivalent circuit corresponding to the proposed filter; the electrical parameters of the equivalent circuit models in this filter are $L_d = 4$ nH, $L_c = 1$ nH, $C_c = 0.97$ PF, $L_s = 0.9$ nH, $C_s = 0.9$ PF, $L_{r1} = 1.35$ nH, $C_{r1} = 1.21$ PF, $L_{r2} = 0.65$ nH, $C_{r2} = 1.52$ PF.

3. MULTIBAND FILTER

One of the proposed structure applications is in filter designing. It is even possible to design a simple high-order filter using n aligned SIW-CSRRs [3–7]. This provides the possibility of designing a filter with specified features, while it is possible to incorporate features such as higher group delay, adjustment of bandwidth, multiband, more selective passband with better out-of-band rejection and higher degree of freedom. However, this ensues higher insertion losses and comparatively less miniaturization.

Structure of resonator proposed in previous part can be operated as a dual-band bandpass filter. With due observance to the said issue, a quad-band bandpass filter with high quality factor can be attained in narrow band by placing two cells of the proposed resonator with different dimensions (according to Figure 7). Note that CSRR 2 as shown in Figure 7 is scaled by a factor of 0.75 compared

with the CSRR 1 to adjust its resonance frequencies. The substrate is Rogers RT/Duroid 5880 as thick as 0.508 mm. The situation of each frequency band can be controlled with the adoption of change in relevant ring slot dimensions. As a matter of fact, each ring slot in quad-band filter structure leads to a passband below cutoff frequency.

The made sample (prototype) of this filter is shown in Figure 8. The results of simulation in "HFSS" software and measurement of this filter are shown in Figure 9. The disagreement in the results of simulation andmeasurement is due to the high sensitivity of some of the ring slots and inadequate precision in their manufacturing process. The results indicate that passing bands in frequencies about 4.7, 5.3, 6.3 and 7.1 GHz are with bandwidths approx. 40, 8, 50 and 10 MHz, respectively while insertion losses stand at approx. 0.6, 3.6, 1 and 2.5 decibels.

Meanwhile, in the quad-band filter proposed in [20], passing bands of the filter stand at 3.82, 5.02, 6.12 and 9.07 GHz while insertion losses stand at 1.77, 3.61, 3.47 and 4.47 decibels, respectively. Special features of the proposed structure compared with other similar structures are as follows: Further miniaturization, low losses, possibility of relatively large tuning one of the passbands of quad-band filter without affecting the other bands, low bandwidth (narrow band).
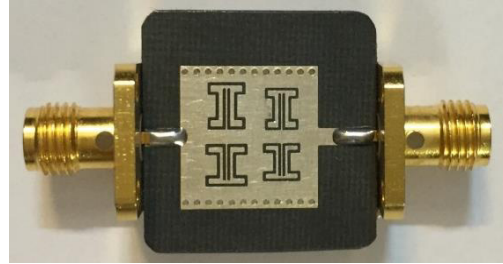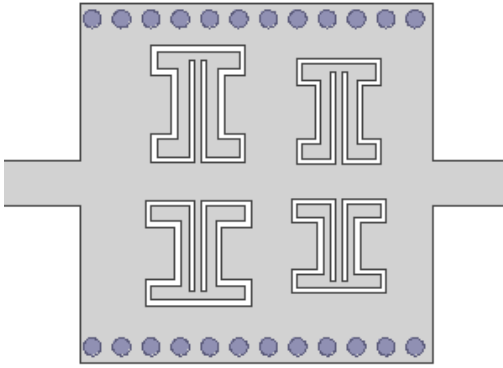
Figure 7. Configuration of the proposed quad-band bandpass filter. The geometrical parameters of CSRR 1 (two ring slots of left side) are similar to the dimensions given in Figure 2. The CSRR 2 (two ring slots of right side) is scaled by a factor of 0.75 compared with the CSRR 1.

Figure 8. Image of the fabricated quad-band bandpass filter.


(a)

(b)
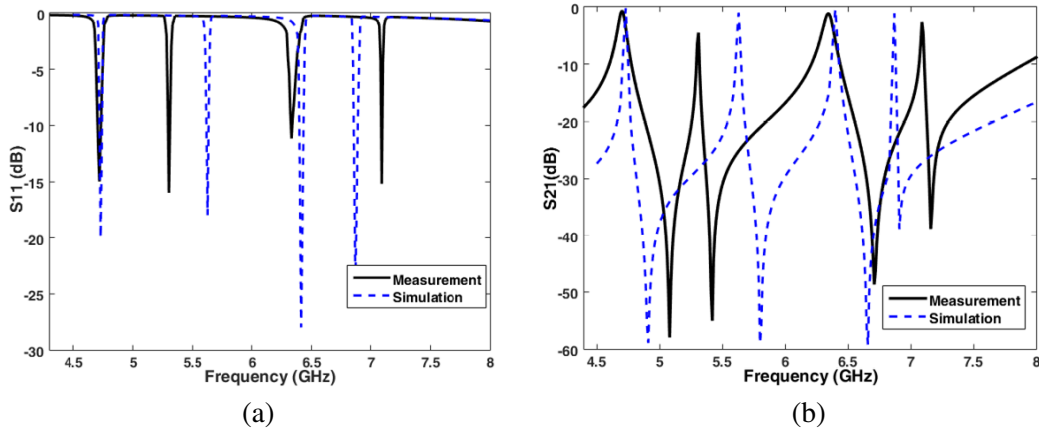
Figure 9. Measured and simulated transmission responses of the proposed quad-band bandpass filter; (a) S_{11} parameter and (b) S_{21} parameter.

4. MULTIBAND DIPLEXER

Diplexer is a key component of telecommunications transceiver which affects performance of system severely. In this part, a planar diplexer will be studied using the proposed CSRR which shows a good performance. This diplexer includes three ports and two continuous filters which are operated below cutoff frequency using SIW technology. After obtaining two dual-band filters with desirable features, the T-junction is designed and optimized. The substrate is Rogers RT/Duroid 5880 as thick as 0.508 mm. The structure of this diplexer is shown in Figure 10 while its fabricated sample is shown in Figure 11. A direct 50 ohm microstrip line inset-feeding is adopted on the top working as the T-junction in order to save the space. This technique, also known as the CPW-SIW transition, is commonly used for impedance matching in the SIW technology. The slot coupling and inset length of the feeding can be used to control the external quality factor.

The results of simulation and measurement of this diplexer are shown in Figure 12. The results indicate that input signal passes from Port 1 to Port 3 with insertion losses stand at approx. 2.5 and 2.8 decibels in frequencies about 4.66 and 5.31 GHz, respectively. Moreover, return losses stand at approx. 19 and 15 decibels. In frequencies about 6.36 and 7.17 GHz, input signal passes from Port 1 to Port 2 with insertion losses at approx. 1.8 and 3 decibels, respectively, while return losses hit approx. 25 and 23.5 decibels. Meanwhile, isolation in all passbands is better than 25 decibels. Thus, the proposed diplexer meets the following criteria: high miniaturizing percentage, high isolation, low losses and the possibility of sending signal in two frequency bands in each of the two routes.
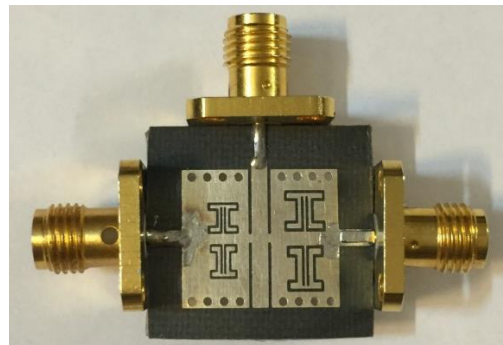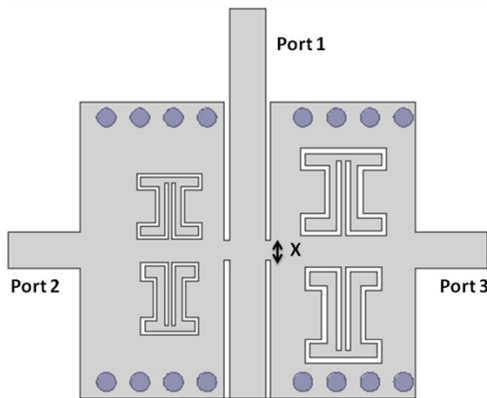
Figure 10. Configuration of the proposed diplexer. The geometrical parameters of ring slots are similar to the dimensions given for the filter in Figure 7.

Figure 11. Image of the fabricated diplexer.
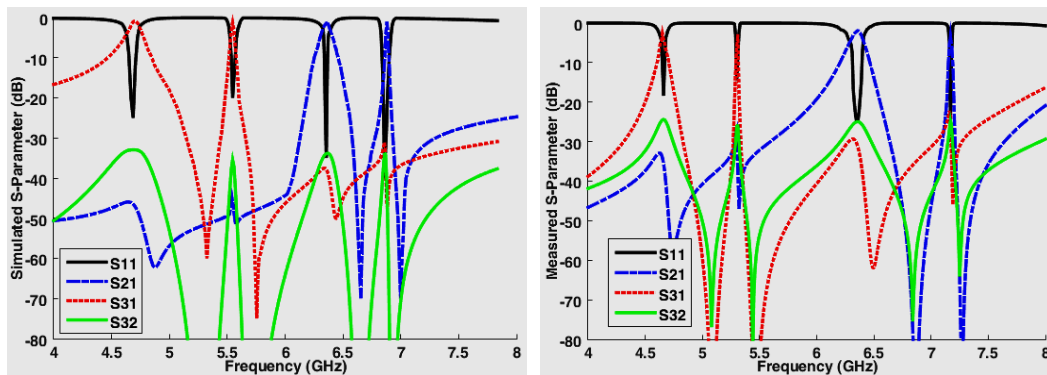
Figure 12. Measured and simulated transmission responses of the proposed diplexer.

Drawing a comparison with the diplexer proposed in [21], it can be concluded that, firstly, this diplexer in each route operates in one only frequency band (unlike diplexer proposed by us which is dual bands), and secondly, insertion losses stand at 1.6 and 2.3 decibels. Thirdly, isolation is about 32 decibels. As a matter of fact, dual-band and higher miniaturizing percentage have been cited as the main specifications of the diplexer as proposed in this paper in comparison with that presented in [21].
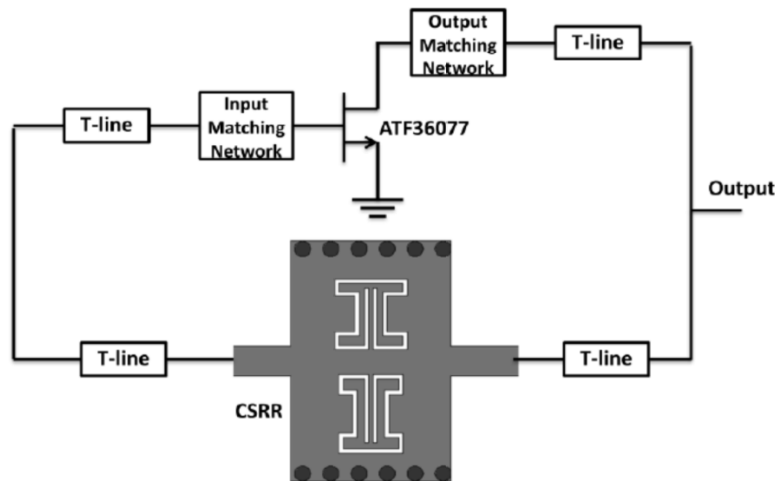
5. LOW PHASE NOISE OSCILLATOR

In this section, a novel low phase noise oscillator using the proposed cavity-backed CSRR resonator is presented. The design procedure and experimental verification are provided in the following.

The first stage for implementing this oscillator is to design a high Q factor resonator done in Section 2. For the purpose of achieving an ultra-low phase noise oscillator, the oscillator designing frequency was considered to be the same as the frequency of the proposed CSRR resonator's second passband (i.e., 5.3 GHz) which enjoyed very high Q-factor and group delay. The second step is to design an active device with ultra-low phase noise, which has proper amplification to start and keep an oscillating. On the other hand, the feedback path's gain which is part of oscillation conditions is provided via the active device.

To minimize the mismatch loss, it is necessary to match the input and output of the active device to the 50 Ohm line. The active device used here is an ATF36077 low noise pseudomorphic high electron-mobility transistor (PHEMT). The length of the microstrip transmission line is used and adjusted for meeting the oscillation condition. Based on Barkhausen oscillation criteria, an oscillator's open loop gain has to be greater than 1 (by adjusting the active device), and the total loop phase has to be 0° or a multiple of 360° (by adjusting the length of T-line). Circuit schematic of the low phase noise oscillator employing the SIW cavity CSRR is shown in Figure 13.

Figure 14 shows a photograph of the fabricated oscillator. The oscillator was measured using a spectrum analyzer Agilent E5504A. The measured oscillation frequency equals 5.36 GHz. It is noted that a small frequency shift is observed which will affect the matching and oscillating condition. Some mechanical tuning using small pieces of copper sheet is performed before achieving the best result. The output power at the oscillation frequency is 7 dBm. Figure 15 plots the simulated (were employed in ADS software) and measured phase noises at the oscillation frequency. It is seen that the two phase noises $-128\frac{\text{dBc}}{\text{Hz}}$ and $-145\frac{\text{dBc}}{\text{Hz}}$ were obtained at offset frequencies 100 KHz and 1 MHz, respectively. The simulation and measurement results for phase noise are in relatively good agreement, except for low offset frequency region. The reason is that simulated oscillator model does not include flicker noise source. Less power consumption can be obtained by choosing a better low noise transistor. One merit of the proposed oscillator, compared to the oscillators reported in the scientific literature [10–19, 22–34],

Figure 13. Circuit schematic of the low phase noise oscillator employing the SIW cavity CSRR resonator.
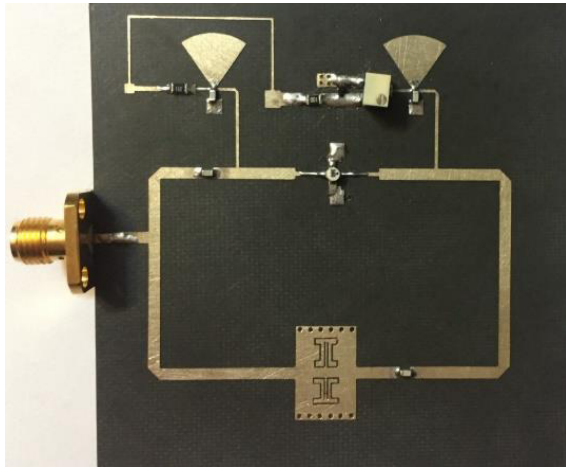
Figure 14. The circuit layout of the fabricated oscillator.
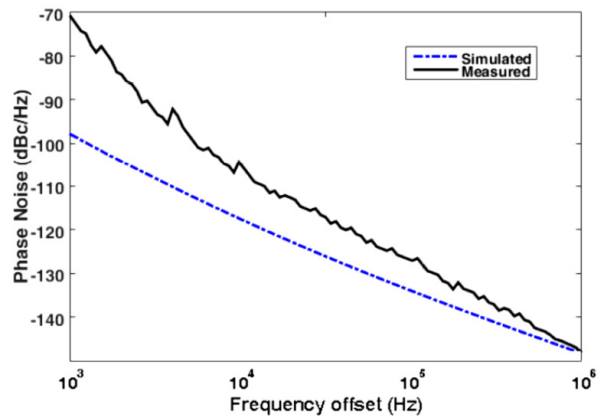
Figure 15. Measured and simulated phase noise for the proposed oscillator.

Table 1. Comparison with other reported microwave planar hybrid oscillator.

Ref.	Resonator	F_0 (GHz)	P_output (dBm)	PN @ 100 KHz (dBc/Hz)
[23]	Hairpin	9	9	-112
[24]	Planar waveguide cavity	15	14	-98
[25]	Substrate waveguide cavity	12	-	-73
[12]	Ring resonator	12	5.33	-96.17
[26]	Microstrip resonator	9.95	7	-113
[13]	Active resonator	10	10.74	-112.05
[27]	Open loop resonator	5.84	-0.5	-113.2
[28]	Elliptic filter	9.05	3.5	-116 (-140 @ 1 MHz)
[29]	Extended resonance	9.1	9.7	-119
[19]	Passive elliptic filter	8.06	3.5	-122.5 (-143.5 @ 1 MHz)
[18]	Passive trisection	2.46	6.4	-120.4 (-144.47 @ 1 MHz)
[15]	complementary spiral resonators	5.74	10.5	-127.5
[17]	Active elliptic filter	8.1	10	~ -124 (-150 @ 1 MHz)
[30]	LC (on chip)	5.38	-4	-127 @ 1 MHz
[16]	Left-handed resonator	21 and 55	14 and -	-100.8 and -86.7 @ 1 MHz
[14]	Cavity-backed CSRR	2.675 and 3.77	5.33 and 10.83	-105.5 and -99.63
[31]	Microstrip resonator	3.36 and 5.24	-9.99 and -15.58	-102.86 and -93.80 @ 10 MHz
[32]	Microstrip resonator	5.7 and 6.48	4.02 and 4.02	-116.3 and -95.23 @ 1 MHz
[33]	SIW-CSRR	4.18 and 5.49	-0.87 and 5.38	-112.3 and -110.3
[34]	Active elliptic filter	8	10	-128 (-150 @ 1 MHz)
This work	SIW cavity-backed CSRR (passive filter)	5.36	7	-128 (-145 @ 1 MHz)

is a record which it set in terms of a phase noise's lowness. Table 1 compares the oscillator proposed in this study and other microwave planar oscillators reported in other articles. It should be noted that the oscillator proposed in [34] has an active resonator with much larger size, and also for designing this oscillator, three transistors are used. Moreover, the noise figure of the transistor used in the feedback loop of this oscillator is much lower.

6. CONCLUSION

In this paper, one modern dual-band CSRR with high quality factor in each of the two bands is introduced, studied and fabricated. High Q factor and its high small-sized percentage is the salient specification of this structure compared to other similar planar resonators proposed in various references. It should be noted that if the loss of the proposed resonator is less than 2 (3) decibel then its unloaded Q factor stands at approx. 1800 (2500). Although there is high possibility of attaining group delay, destructive effects of insertion losses are impeded. As a matter of fact, there is a trade-off between increased group delay and reduced insertion losses in passband.

Then, a small low-loss narrow-band quad-band filter and a small low-loss dual-band diplexer with isolation better than 25 decibels are introduced and fabricated using this resonator. This resonator is also very suitable for designing a low phase noise oscillator. Thus, an ultra-low phase noise oscillator of parallel feedback type is designed and fabricated. The results reveal that at the oscillation frequency 5.36 GHz, $-128\frac{\text{dBc}}{\text{Hz}}$ phase noise is obtained at 100 KHz offset frequency and $-145\frac{\text{dBc}}{\text{Hz}}$ at 1 MHz offset frequency. Compared to the oscillators reported in the scientific literature, the proposed oscillator sets a record in terms of a phase noise's lowness.

REFERENCES

1. Caloz, C. and A. Rennings, "Overview of resonant metamaterial antennas," *3rd European Conference on Antennas and Propagation, 2009. EuCAP 2009*, 615, 619, March 23–27, 2009.
2. Baena, J. D., J. Bonache, F. Martin, R. M. Sillero, F. Falcone, T. Lopetegi, M. A. G. Laso, J. Garcia-Garcia, I. Gil, M. F. Portillo, and M. Sorolla, "Equivalent-circuit models for split-ring resonators and complementary split-ring resonators coupled to planar transmission lines," *IEEE Transactions on Microwave Theory and Techniques*, Vol. 53, No. 4, 1451, 1461, April 2005.
3. Dong, Y. D., T. Yang, and T. Itoh, "Substrate integrated waveguide loaded by complementary split-ring resonators and its applications to miniaturized waveguide filters," *IEEE Transactions on Microwave Theory and Techniques*, Vol. 57, No. 9, 2211, 2223, September 2009.
4. Cui, Y., L. Jin, Z. Zhang, and L. Li, "Novel design of substrate integrated waveguide filter employing broadside-coupled complementary split ring resonators," *IEICE Electronics Express*, Vol. 12, No. 6, 20150188, 2015.
5. Zhang, X.-C., Z.-Y. Yu, and J. Xu, "Novel band-pass substrate integrated waveguide (SIW) filter based on complementary split ring resonators (CSRRs)," *Progress In Electromagnetics Research*, Vol. 72, 39–46, 2007.
6. Dong, Y. and T. Itoh, "Miniaturized dual-band substrate integrated waveguide filters using complementary split-ring resonators," *2011 IEEE MTT-S International Microwave Symposium Digest (MTT)*, 1, June 5–10, 2011.
7. Zhang, Q.-L., W.-Y. Yin, S. He, and L.-S. Wu, "Evanescent-mode substrate integrated waveguide (SIW) filters implemented with complementary split ring resonators," *Progress In Electromagnetics Research*, Vol. 111, 419–432, 2011.
8. Dong, Y. D. and T. Itoh, "Miniaturized substrate integrated waveguide slot antennas based on negative order resonance," *IEEE Transactions on Antennas and Propagation*, Vol. 58, No. 12, 3856, 3864, December 2010.
9. Hong, J.-S. G. and M. J. Lancaster, *Microstrip Filters for RF/Microwave Applications*, John Wiley & Sons, Inc., 2001.
10. Ha, S. J., Y. D. Lee, Y. H. Kim, J. J. Choi, and U. S. Hong, "Dielectric resonator oscillator with balanced low noise amplifier," *Electronics Letters*, Vol. 38, No. 24, 1542, 1544, November 21, 2002.
11. Du, Y., Z.-X. Tang, B. Zhang, and P. Su, "K-band harmonic dielectric resonator oscillator using parallel feedback structure," *Progress In Electromagnetics Research Letters*, Vol. 34, 83–90, 2012.
12. Hsieh, L.-H. and K. Chang, "High-efficiency piezoelectric-transducer-tuned feedback microstrip ring-resonator oscillators operating at high resonant frequencies," *IEEE Transactions on Microwave Theory and Techniques*, Vol. 51, No. 4, 1141, 1145, April 2003.

13. Lee, Y.-T., J. Lee, and S. Nam, "High-Q active resonators using amplifiers and their applications to low phase-noise free-running and voltage-controlled oscillators," *IEEE Transactions on Microwave Theory and Techniques*, Vol. 52, No. 11, 2621, 2626, November 2004.

14. Dong, Y. D. and T. Itoh, "A dual-band oscillator with reconfigurable cavity-backed complementary split-ring resonator," *2012 IEEE MTT-S International Microwave Symposium Digest (MTT)*, 1, 3, June 17–22, 2012.

15. Choi, J. and C. Seo, "High-Q metamaterial interdigital transmission line based on complementary spiral resonators for low phase noise voltage-controlled oscillator," *IET Circuits, Devices & Systems*, Vol. 6, No. 3, 168, 175, May 2012.

16. Yu, A. H.-T., S.-W. Tam, Y. Kim, E. Socher, W. Hant, M.-C. F. Chang, and T. Itoh, "A dual-band millimeter-wave cmos oscillator with left-handed resonator," *IEEE Transactions on Microwave Theory and Techniques*, Vol. 58, No. 5, 1401, 1409, May 2010.

17. Nick, M. and A. Mortazawi, "Oscillator phase-noise reduction using low-noise high-Q active resonators," *2010 IEEE MTT-S International Microwave Symposium Digest (MTT)*, 276, 279, May 23–28, 2010.

18. Chang, C.-L. and C.-H. Tseng, "Design of low phase-noise oscillator and voltage-controlled oscillator using microstrip trisection bandpass filter," *IEEE Microwave and Wireless Components Letters,*, Vol. 21, No. 11, 622, 624, November 2011.

19. Choi, J., M. Nick, and A. Mortazawi, "Low phase-noise planar oscillators employing elliptic-response bandpass filters," *IEEE Transactions on Microwave Theory and Techniques*, Vol. 57, No. 8, 1959, 1965, August 2009.

20. Dong, Y. D., C. T. M. Wu, and T. Itoh, "Miniaturised multi-band substrate integrated waveguide filters using complementary split-ring resonators," *IET Microwaves, Antennas & Propagation*, Vol. 6, No. 6, 611–620, April 24, 2012.

21. Dong, Y. D. and T. Itoh, "Substrate integrated waveguide loaded by complementary split-ring resonators for miniaturized diplexer design," *IEEE Microwave and Wireless Components Letters*, Vol. 21, No. 1, 10–12, January 2011.

22. Zhang, X.-C., Z.-Y. Yu, and J. Xu, "Novel band-pass substrate integrated waveguide (SIW) filter based on complementary split ring resonators (CSRRs)," *Progress In Electromagnetics Research*, Vol. 72, 39–46, 2007.

23. Dussopt, L., D. Guillois, and G. M. Rebeiz, "A low phase noise silicon 9 GHz VCO and an 18 GHz push-push oscillator," *2002 IEEE MTT-S International Microwave Symposium Digest*, Vol. 2, 695–698, June 2–7, 2002.

24. Lee, W.-C., S.-C. Lin, and C.-K. C. Tzuang, "Planar realization of low phase noise 15/30 GHz oscillator/doubler using surface mount transistors," *IEEE Microwave and Wireless Components Letters*, Vol. 13, No. 1, 10–12, January 2003.

25. Cassivi, Y. and K. Wu, "Low cost microwave oscillator using substrate integrated waveguide cavity," *IEEE Microwave and Wireless Components Letters*, Vol. 13, No. 2, 48–50, February 2003.

26. Khanna, A. P. S., E. Topacio, E. Gane, and D. Elad, "Low jitter silicon bipolar based VCOs for applications in high speed optical communication systems," *2001 IEEE MTT-S International Microwave Symposium Digest*, Vol. 3, 1567–1570, May 20–24, 2001.

27. Park, E. and C. Seo, "Low phase noise oscillator using microstrip square open loop resonator," *IEEE MTT-S International Microwave Symposium Digest, 2006*, 585–588, June 11–16, 2006.

28. Choi, J., M.-H. Chen, and A. Mortazawi, "An X-band low phase noise oscillator employing a four-pole elliptic-response microstrip bandpass filter," *IEEE/MTT-S International Microwave Symposium, 2007*, 1529–1532, June 3–8, 2007.

29. Choi, J. and A. Mortazawi, "A new X-band low phase-noise multiple-device oscillator based on the extended-resonance technique," *IEEE Transactions on Microwave Theory and Techniques*, Vol. 55, No. 8, 1642–1648, August 2007.

30. Victor, A. and M. B. Steer, "Reflection coefficient shaping of a 5-GHz voltage-tuned oscillator for improved tuning," *IEEE Transactions on Microwave Theory and Techniques*, Vol. 55, No. 12, 2488–2494, December 2007.

31. Iyer, B., A. Kumar, and N. P. Pathak, "3.36-/15.24-GHz concurrent dual-band oscillator for WiMAX/WLAN applications," *IEEE MTT-S International Microwave and RF Conference*, 1–4, New Delhi, 2013.

32. Sharma, V., R. Yadav, and N. P. Pathak, "Series switched resonator based dual-band oscillator," *General Assembly and Scientific Symposium, 2011 30th URSI*, 1–4, Istanbul, 2011.

33. Yang, Z., J. Dong, B. Luo, T. Yang, and Y. Liu, "Low phase noise concurrent dual-band oscillator using compact diplexer," *IEEE Microwave and Wireless Components Letters*, Vol. 25, No. 10, 672–674, October 2015.

34. Nick, M. and A. Mortazawi, "Low phase-noise planar oscillators based on low-noise active resonators," *IEEE Transactions on Microwave Theory and Techniques*, Vol. 58, No. 5, 1133–1139, May 2010.